Nanoscale

PAPER

View Article Online
View Journal | View Issue

Cite this: *Nanoscale*, 2017, **9**, 850

δ-Phosphorene: a two dimensional material with a highly negative Poisson's ratio†

Haidi Wang,[a] Xingxing Li,[a,b] Pai Li[a] and Jinlong Yang*[a,b]

Received 2nd November 2016,
Accepted 28th November 2016

DOI: 10.1039/c6nr08550d

www.rsc.org/nanoscale

As a basic mechanical parameter, Poisson's ratio (ν) measures the mechanical responses of solids against external loads. In rare cases, materials have a negative Poisson's ratio (NPR), and present an interesting auxetic effect. That is, when a material is stretched in one direction, it will expand in the perpendicular direction. To design modern nanoscale electromechanical devices with special functions, two dimensional (2D) auxetic materials are highly desirable. In this work, based on first principles calculations, we rediscover the previously proposed δ-phosphorene (δ-P) nanosheets [Jie Guan, *et al.*, *Phys. Rev. Lett.*, 2014, **113**, 046804] which are good auxetic materials with a high NPR. The results show that the Young's modulus and Poisson's ratio of δ-P are all anisotropic. The NPR value along the grooved direction is up to −0.267, which is much higher than the recently reported 2D auxetic materials. The auxetic effect of δ-P originating from its puckered structure is robust and insensitive to the number of layers due to weak interlayer interactions. Moreover, δ-P possesses good flexibility because of its relatively small Young's modulus and high critical crack strain. If δ-P can be synthesized, these extraordinary properties would endow it with great potential in designing low dimensional electromechanical devices.

1 Introduction

Poisson's ratio and Young's modulus are of great importance to evaluate a material's mechanical strength and stability,[1–5] and also crucial to design high performance electromechanical devices. Poisson's ratio (ν),[6–8] defined as the ratio of the strain in the transverse direction to that of the longitudinal direction, measures the fundamental mechanical responses of solids against external loads. In general, when a compressive (tensile) stress is acted in one direction, materials tend to expand (contract) in the perpendicular direction. For these materials, Poisson's ratio has a positive value. The Poisson's ratios of common solid state crystals usually fall in the range of $0 < \nu < 0.5$, while gases and cork[9,10] have $\nu \approx 0$. In rare cases, a negative Poisson's ratio (NPR)[7] is attainable, which shows a strong correlation with atomic packing density, atomic connectivity[8] and structural phase transition.[11,12] These materials are called auxetic materials, and typically have enhanced toughness and shear resistance, as well as significant sound and vibration absorption. Auxetic materials have been exploited in fields such as medicine, fasteners, tougher composites, national security and defense.[13]

So far, the search for NPR materials has mainly been focused on bulk and engineered auxetic structures. In 1987, foams with negative Poisson's ratios were firstly produced by Lakes[14] from conventional low density open-cell polymer foams by causing the ribs of each cell to permanently protrude inward. For this auxetic material, the NPR arises from its re-entrant structure. Later, auxetic phenomena have also been observed in crystalline SiO_2 and other cubic materials.[15–18]

To fabricate electromechanical devices at the nanoscale, low dimensional auxetic materials are very desirable. In recent years, there has been increasing interest in exploring the possibility of auxetic phenomenon in low dimensional systems.[1,13,19–22] For example, theoretical calculation has forecasted that black phosphorene (BP)[23] possesses an intrinsic auxetic effect resulting from its puckered configuration,[1] although the NPR value is comparatively small (−0.027). In addition, auxetic phenomena have also been predicted in borophene,[20] penta-graphene,[24] penta-B_2N_4,[22] Be_5C_2 [25] and SnSe.[19] However, the NPR values of all these 2D materials are relatively small, hindering their further applications. In order to design high performance nanoscale electromechanical devices, 2D materials with high NPRs are urgently needed.

[a]*Hefei National Laboratory for Physical Sciences at the Microscale, University of Science and Technology of China, Hefei, Anhui 230026, China. E-mail: jlyang@ustc.edu.cn*
[b]*Synergetic Innovation Center of Quantum Information & Quantum Physics, University of Science and Technology of China, Hefei, Anhui 230026, China*

† Electronic supplementary information (ESI) available: Phonon bands of δ-P at the different uniaxial strain; the wireframe sketch of δ-P and BP; stacking order and relative energy for multilayer δ-P; band structure, band decomposed charge density and DOS of primitive δ-P and strain engineers; the elastic constants for mono-layered δ-P; the calculated elastic stiffness constants for bulk δ-P. See DOI: 10.1039/c6nr08550d

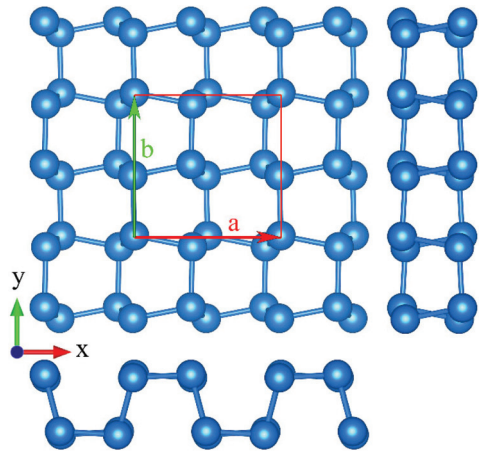

Fig. 1 The top and side views of the relaxed δ-P. The directions of two basis vectors *a* and *b* of the unit cell are indicated.

In this work, based on first-principles calculations, we further study the orientation-dependent Young's modulus, Poisson's ratio, quantum size effect and electronic structure of previously proposed δ-P (see Fig. 1).[26] Interestingly, we discover that δ-P is a superior auxetic material with a NPR value as large as −0.267. Like its allotrope BP,[3] δ-P has a puckered structure with grooves formed by two layers of phosphorus atoms. A previous study[26] demonstrates that δ-P is stable up to 1000 K. Besides, δ-P has good electronic properties. For example, the band gap of δ-P is 0.66 eV (HSE06 level),[27] which indicates that δ-P has a potential application for designing nano electro-optical devices with infrared light absorption.

2 Methods

The first principles calculations were carried out based on the Kohn–Sham density functional theory[28] (KS-DFT) as implemented in the Vienna *ab initio* simulation package (VASP).[29] The generalized gradient approximation as parameterized by Perdew, Burke and Ernzerhof[30] (PBE) for exchange–correlation functional was used. Electronic wave functions were expanded in a plane wave basis set with a kinetic energy cutoff of 450 eV. The convergence criterion for the energy in electronic SCF iterations and the force in ionic step iterations were set to 1.0×10^{-6} eV and 5.0×10^{-3} eV Å^{-1}, respectively. The non-periodic direction was set along the *z* direction and an at least 15 Å vacuum slab was added to eliminate the interaction between δ-P and its replicas that resulted from the periodic boundary conditions. The reciprocal space was sampled with a *k*-grid density of $0.04 \times 2\pi$ Å^{-1} for the ionic iterations and $0.02 \times 2\pi$ Å^{-1} for electronic SCF iterations using the Monkhorst–Pack method. Besides, a van der Waals[31–33] (vdW) correction proposed by Grimme (DFT-D2) was chosen due to its good description of long-range vdW interactions. Phonon properties were calculated using a finite displacement method implemented in Phonopy.[34] A 3 × 3 supercell was constructed to calculate the atomic forces by using VASP, with a relatively high accuracy.

To calculate the mechanical properties of materials, such as elastic constants, the ideal strength, Young's modulus and Poisson's ratio, we developed a python general elastic calculation (PyGEC) package. For a 2D material, the stress–strain equation is obtained from Hooke's law [eqn (1)] under plane-stress condition.[35]

$$\begin{bmatrix} \sigma_{xx} \\ \sigma_{yy} \\ \sigma_{xy} \end{bmatrix} = \begin{bmatrix} C_{11} & C_{12} & 0 \\ C_{12} & C_{22} & 0 \\ 0 & 0 & C_{66} \end{bmatrix} \begin{bmatrix} \varepsilon_{xx} \\ \varepsilon_{yy} \\ 2\varepsilon_{xy} \end{bmatrix} \quad (1)$$

We scanned the energy surface of materials in the strain range $-1.5\% < \varepsilon_{xx} < 1.5\%$, $-1.5\% < \varepsilon_{yy} < 1.5\%$ and $-1.0\% < \varepsilon_{xy} < 1.0\%$. The strain mesh grid was set to be 7 × 7 × 5. For 2D orthorhombic structures, the calculated four elastic stiffness constants C_{11}, C_{12}, C_{22}, C_{66} (ESI, Table S1†), satisfy the necessary mechanical equilibrium conditions[36] for mechanical stability: $C_{11}C_{22}-C_{12}^{2} > 0$ and C_{11}, C_{22}, $C_{66} > 0$. Then, the orientation-dependent Young's modulus $E(\theta)$ and Poisson's ratio $\nu(\theta)$ were calculated as:[3]

$$\begin{cases} E(\theta) = \dfrac{Y_{zz}}{\cos^4\theta + d_2\cos^2\theta\sin^2\theta + d_3\sin^4\theta} \\ \nu(\theta) = \dfrac{\nu_{zz}\cos^4\theta - d_1\cos^2\theta\sin^2\theta + \nu_{zz}\sin^4\theta}{\cos^4\theta + d_2\cos^2\theta\sin^2\theta + d_3\sin^4\theta} \end{cases} \quad (2)$$

where d_1, d_2, d_3, Y_{zz} and ν_{zz} are elastic constant related variables (ESI, eqn (S1)†). For bulk structure, we employed PyGEC to calculate the elastic constant C_{ij},[37–39] and then used the ElAM[40] code to analyze the Young's modulus and Poisson's ratio.

3 Results and discussion

The rectangular Wigner–Seitz cell of δ-P contains 8 atoms with $Pmc2_1$ symmetry. Our calculated lattice parameters for δ-P are $a = 5.50$ Å and $b = 5.40$ Å, consistent with a previous theoretical study.[26] To explore the ideal tensile strength (the highest achievable stress of a defect-free crystal at 0 K) and critical strain (the strain at which ideal strength reaches)[41] of δ-P, an in-plane uniaxial tensile force is applied along either the *x* or the *y* direction. The stress–strain relationship for monolayer δ-P is presented in Fig. 2(a), where the tensile strain ranges from 0 to 30%. The ideal strengths are 7.08 GPa and 14.06 GPa in the *x* and *y* directions, respectively. The corresponding critical strains are almost of the same value (18.95%). We note that phonon instability may occur before mechanical failure. Such a failure mechanism has been well studied in graphene where the phonon softening induced by Kohn anomaly occurs before the stress reaches its maximum.[42,43] To check the dynamic stability, we have calculated the phonon band structure with external strains applied along the *x* and *y* directions (see Fig. S1 in ESI†), respectively. The results demonstrate that a strain up to 18.95% (equivalent to the mechanical fracture strength) along the *y* direction is accessible whilst sustaining

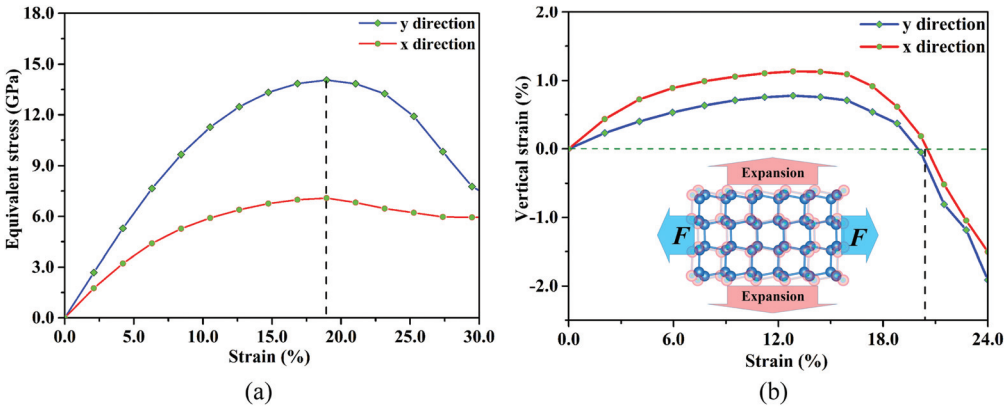

Fig. 2 (a) The strain–stress relation for monolayer δ-P. The strain is defined as $(r - r_0)/r_0$, where r_0 is the equilibrium lattice and r stands for the strained one. The vertical dashed line indicates the critical strain and ideal strength. (b) The induced vertical strain in the x direction when tensile strain is applied along the y direction (red line). The blue one is for vertical strain along the y direction. The vertical dashed line indicates the Poisson's ratio that is converted to the normal one.

good phonon stability. As for the x direction, when the strain reaches 18.95%, a relatively large imaginary frequency occurs. However, according to our calculations, δ-P can bear at least a strain of 15% along the x direction.

Generally speaking, when a material is stretched in one direction, it tends to contract in the perpendicular direction. That is, when tensile force is applied along one direction, the resulting vertical strain will be negative. This phenomenon is named the positive Poisson effect. However, for δ-P, we find that the tensile force [F, the insert of Fig. 2(b)] along the x direction leads to a positive vertical strain along the y direction, with the strain up to around 20%. So does the y direction. These results strongly indicate that δ-P has an anomalous auxetic effect with NPRs. What is more, the auxetic effect exists in a large strain range. In particular, this effect can be sustained along the y direction until the cracking of the 2D material, since the critical strain (18.95%) is smaller than 20%.

In the above section, we have gained a basic look into the mechanical response of δ-P by considering a uniaxial deformation only in the x- or y-direction. However, due to the anisotropic geometric structure, the mechanical properties of δ-P are expected to be also highly orientation-dependent. In order to get a full understanding of the mechanical properties of δ-P, the orientation-dependent Young's modulus and Poisson's ratio are calculated [Fig. 3(a) and (b)]. The Young's modulus represents the fully reversible stiffness response as in a linear elastic Hookean spring.[44] The 2D polar representation curve in Fig. 3(a) clearly indicates that the Young's modulus of δ-P is highly anisotropic, just as expected. The Young's modulus along the y direction has a maximal value of 142.86 GPa and the minimum value of 62.28 GPa occurs along the direction indicated by a red arrow. For the x direction, it has a median value of 84.87 GPa. We notice that the maximal/minimal Young's modulus of δ-P and BP have similar values, which may arise from their similar geometric structures. On the other hand, since the P–P bond strength is weak and the compromised dihedral angles rather than the bond length stretch under tensile force, the Young's modulus of both BP and δ-P are much smaller than those of graphene (1.0 TPa), MoS_2 (0.33 TPa) and BN (0.25 TPa),[2,45–47] which suggests that 2D δ-P is as flexible as BP.

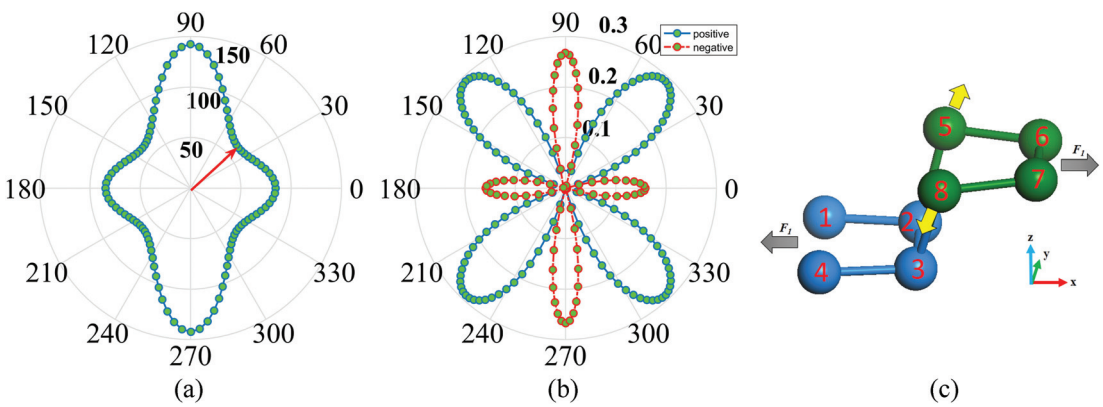

Fig. 3 Calculated orientation-dependent (a) the Young's modulus $E(\theta)$ in GPa, (b) Poisson's ratio $\nu(\theta)$. (c) The evolution of the local structure of δ-P under tensile force (F_1) along the x direction. δ-P expands along the y direction, indicated by yellow arrows.

From Fig. 3(b), one can see that the Poisson's ratios for δ-P are also spatially varying. In particular, δ-P exhibits a negative Poisson's ratio along the x, y and their neighboring directions, while in the directions away from x and y, δ-P presents a normal positive Poisson's ratio. The maximal negative and positive Poisson's ratios are −0.267 and 0.29 along the y direction and the diagonal direction, respectively. As a comparison, we list the NPR values of recently reported 2D materials in Table 1. The NPR values of these 2D materials in the references were calculated by PBE functional, except for the bilayer-graphene's (VDW functional). We firstly recalculate the Poisson's ratio of all these selected 2D systems by using the PBE functional. The result shows that most of the Poisson's ratio values are negative and approximately equal to the reference ones, which further demonstrates the validity of our calculations. However, due to the special origin of NPR in bilayer-graphene,[13] the Poisson's ratio value calculated by PBE is positive (against the reference one), which proves to be wrong, since PBE gives a rather poor description of weak interlayer interaction in bilayer graphene. Considering that the NPR values are possibly affected by the exchange and correlation functional forms, the VDW-DF functional[48,49] is employed to recalculate their Poisson's ratio values. As listed in Table 1, a NPR is obtained for bilayer-graphene. What's more, the variation trend of the NPRs calculated with the VDW-DF functional is similar to those with PBE. In this work, the NPR of δ-P calculated with PBE functional will be adopted. According to Table 1, it can be concluded that δ-P has the highest NPR value among these auxetic materials. It is also worth noting that the auxetic effect of BP[1] and bilayer-graphene[13] exists only along one direction, while δ-P holds for both the x and y directions.

Due to the similarity between the geometric structures of δ-P and BP, we may explain the origin of the auxetic effect of δ-P in a similar way.[1] We plot the local skeleton structure of monolayer δ-P in Fig. 3(c), where the direction of the tensile force and the motion of atoms are illustrated. Taking tensile force F_1 in the x direction as an example, the four top-most atoms 5, 6, 7 and 8 will move along the right arrow under the force. At the same time, the four bottom-most atoms 1, 2, 3 and 4 will move along the left arrow, which will lead to an increase in angles φ_{125}, φ_{438}, φ_{387} and φ_{652} and strain energy will be stored in these four angles. To accommodate the elongation in the x direction, δ-P will contract along the z direction. That is, atoms 1, 2, 3 and 4 will move upwards and atoms 5, 6, 7 and 8 will move downwards. For ε_{xx} = 0.015, we find the thickness of monolayer δ-P is 2.214 Å, which is smaller than the initial value (2.238 Å). As a consequence, the 3–8 and 2–5 bonds become shorter, and part of the strain energy will be transferred to these bonds. This is an unstable middle state, and a certain procedure is needed to release the strain energy. By carefully examining the original and final structures, we find that the angle φ_{325} reduces by 0.206° while φ_{832} increases by 0.585°. The net effect is that the distance between atom 5 and 8 becomes longer, which leads to the occurrence of an auxetic effect.

Although both δ-P and BP have a honeycomb-like structure, the direction the auxetic effect holds in is different. To illustrate the subtle difference, we draw the wireframe sketches of δ-P and BP (see Fig. S2 in ESI†). The side view indicates that the atoms in the top layer of δ-P have a distortion of about 0.123 Å, and so do the bottom ones. However, no distortion is observed in BP. Because of their structure difference, the anisotropic ratio (defined by E_y/E_x) of BP $(4.013)^3$ is much larger than that of the δ-P's (1.683). In addition, the Poisson's ratio of BP along the groove direction is about 4 times larger than the perpendicular direction. As a consequence, the tensile force along the groove direction of BP will lead to a dramatic contraction on the perpendicular direction. To accommodate the contraction in this direction, the out-of-plane auxetic phenomenon occurs in BP, which has been demonstrated in the experiment.[50] By contrast, the out-of-plane auxetic phenomenon of δ-P is suppressed by a relatively small anisotropic ratio and appropriate in-plane auxetic effects.

Apart from BP, blue phosphorene has been synthesized on a Au(111) surface,[51] however, a theoretical study[52] predicted that it possesses no auxetic effect because no classic re-entrant structure exists. By investigating these 2D materials with NPR, it can be found that the auxetic effect is closely related to the atomic packing density and atom connectivity. Taking BP,[1] SnSe[19] and δ-P as examples, we may find that all these 2D materials share a similar hinge-like structure and this special structure is the necessary condition for their NPR. Thus, to synthesize other 2D phosphorene allotropes with NPR, special attention should be paid to those with BP-like structures.

To investigate the possible quantum size effect on the mechanical properties of δ-P, we also calculate the Young's modulus and Poisson's ratios of double-, triple-, quadruple-layered and bulk δ-P. Firstly, we start with the relaxed monolayer δ-P structure, and explore their possible stacking orders (see Fig. S3 in ESI†). The most favorable stacking configuration is found to be AB-stacking for double-layered δ-P, ABA-stacking for triple-layered δ-P, ABAB-stacking for quadruple-layered δ-P and AB-stacking for bulk δ-P. Then, the mechanical properties of multilayer and bulk δ-P with the most stable stacking configurations are calculated. As listed in Table 2, it can be summarized as follows: (1) the values of the Young's modulus and Poisson's ratio are insensitive to the number of layers. This is because the interaction between the δ-P layers is weak van der Waals interaction with no bonds formed. (2) The NPR along

Table 1 Comparison of negative Poisson's ratios (ν) in recently predicted 2D materials with different functional

System	References	PBE	VDW-DF
δ-P	—	−0.267	−0.400
BP	−0.03 (PBE[1])	−0.048	−0.130
Penta-graphene	−0.07 (PBE[24])	−0.080	−0.075
Bilayer-graphene	−0.10 (VDW[13])	0.642	−0.198
Borophene	−0.04 (PBE[21])	−0.040	−0.032
Penta-B_2N_4	−0.02 (PBE[22])	−0.030	−0.052
SnSe	−0.17 (PBE[19])	−0.201	−0.205

Table 2 The calculated Young's modulus and Poisson's ratios for mono-, double-, triple-, quadruple-layered and bulk δ-P with PBE DFT-D2 functional. ν_{xy} is the Poisson's ratio with tensile strain applied in the *x* direction and the response strain in the *y* direction

	Young's modulus/GPa		Poisson's ratio	
Layers	E_x	E_y	ν_{xy}	ν_{yx}
Mono	84.87	142.86	−0.158	−0.267
Double	89.83	150.37	−0.125	−0.209
Triple	89.55	148.49	−0.128	−0.213
Quadruple	90.55	148.32	−0.129	−0.211
Bulk	89.74	145.42	−0.132	−0.214

the *x* and *y* directions exists in all the cases, indicating that the auxetic effect of δ-P is robust. (3) All structures have a relatively small Young's modulus, with E_y much larger than E_x.

In addition, the electronic structures in response to mechanical stress are also discussed in the ESI.† The calculations show that a semiconductor-metal (M) transition can be observed by only changing the stress direction, and a direct semiconductor (D) to indirect semiconductor (I) transition can also be realized (ESI, Fig. S4 and S5†).

4 Summary

In conclusion, first principles calculations have revealed that δ-P possesses highly anisotropic mechanical properties as well as fascinating characters of auxetic effects. The NPR value is higher than the previously reported 2D materials. The auxetic effect originating from the puckered structure exists in both *x* and *y* directions, and is insensitive to the number of stacked δ-P layers due to the weak van der Waals interaction. Besides, compared to other 2D materials, δ-P has a low Young's modulus and big critical crack strain, which indicates that 2D δ-P is also a material with good flexibility. These superior mechanical properties, along with the tunability of the band gap, the direct-to-indirect semiconductor transition and semiconductor-to-metal transition, make δ-P a promising material for the design of nano-electromechanical devices, and we hope our study will stimulate further experimental effort in this subject.

Acknowledgements

This paper is financially supported by the National Key Research & Development Program of China (Grant No. 2016YFA0200604), by the National Natural Science Foundation of China (NSFC) (Grants No. 21421063, No. 21233007, and No. 21603205), by the Chinese Academy of Sciences (CAS) (Grant No. XDB01020300), by the Fundamental Research Funds for the Central Universities (Grant No. WK2060030023), by the China Postdoctoral Science Foundation (Grant No. BH2060000033). We used computational resources of the Super-computing Center of the University of Science and Technology of China, the Supercomputing Center of the Chinese Academy of Sciences, Tianjin and Shanghai Supercomputer Centers.

References

1 J.-W. Jiang and H. S. Park, *Nat. Commun.*, 2014, **5**, 4727.
2 Q. Wei and X. Peng, *Appl. Phys. Lett.*, 2014, **104**, 251915.
3 L. Wang, A. Kutana, X. Zou and B. I. Yakobson, *Nanoscale*, 2015, **7**, 9746–9751.
4 L. Kou, C. Chen and S. C. Smith, *J. Phys. Chem. Lett.*, 2015, **6**, 2794–2805.
5 F. Hao and X. Chen, *J. Appl. Phys.*, 2015, **118**, 234304.
6 P. H. Mott and C. M. Roland, *Phys. Scr.*, 2013, **87**, 55404.
7 L. D. Landau and E. M. Lifshitz, *Theory of Elasticity*, 3rd edn, 1986.
8 T. Rouxel, *J. Am. Ceram. Soc.*, 2007, **90**, 3019–3039.
9 H. Gercek, *Int. J. Rock Mech. Min. Sci.*, 2007, **44**, 1–13.
10 G. N. Greaves, A. L. Greer, R. S. Lakes and T. Rouxel, *Nat. Mater.*, 2011, **10**, 823–837.
11 P. H. Poole, *Science*, 1997, **275**, 322–323.
12 G. N. Greaves, M. C. Wilding, S. Fearn, D. Langstaff, F. Kargl, S. Cox, Q. V. Van, O. Majérus, C. J. Benmore, R. Weber, C. M. Martin and L. Hennet, *Science*, 2008, **322**, 566–570.
13 S. Woo, H. C. Park and Y.-W. Son, *Phys. Rev. B: Condens. Matter*, 2016, **93**, 75420.
14 R. Lakes, *Science*, 1987, **235**, 1038–1040.
15 F. Milstein and K. Huang, *Phys. Rev. B: Condens. Matter*, 1979, **19**, 2030–2033.
16 N. R. Keskar and J. R. Chelikowsky, *Nature*, 1992, **358**, 222–224.
17 E. A. Friis, R. S. Lakes and J. B. Park, *J. Mater. Sci.*, 1988, **23**, 4406–4414.
18 R. H. Baughman, J. M. Shacklette, A. A. Zakhidov and S. Stafstro, *Nature*, 1998, **392**, 362–365.
19 L.-C. Zhang, G. Qin, W.-Z. Fang, H.-J. Cui, Q.-R. Zheng, Q.-B. Yan and G. Su, *Sci. Rep.*, 2016, **6**, 19830.
20 X.-F. Zhou, X. Dong, A. R. Oganov, Q. Zhu, Y. Tian and H.-T. Wang, *Phys. Rev. Lett.*, 2014, **112**, 85502.
21 A. J. Mannix, X.-F. Zhou, B. Kiraly, J. D. Wood, D. Alducin, B. D. Myers, X. Liu, B. L. Fisher, U. Santiago, J. R. Guest, M. J. Yacaman, A. Ponce, A. R. Oganov, M. C. Hersam and N. P. Guisinger, *Science*, 2015, **350**, 1513–1516.
22 M. Yagmurcukardes, H. Sahin, J. Kang, E. Torun, F. M. Peeters and R. T. Senger, *J. Appl. Phys.*, 2015, **118**, 104303.
23 L. Li, Y. Yu, G. J. Ye, Q. Ge, X. Ou, H. Wu, D. Feng, X. H. Chen and Y. Zhang, *Nat. Nanotechnol.*, 2014, **9**, 372–377.
24 S. Zhang, J. Zhou, Q. Wang, X. Chen, Y. Kawazoe and P. Jena, *Proc. Natl. Acad. Sci. U. S. A.*, 2015, **112**, 2372–2377.
25 Y. Wang, F. Li, Y. Li and Z. Chen, *Nat. Commun.*, 2016, **7**, 11488.
26 J. Guan, Z. Zhu and D. Tomanek, *Phys. Rev. Lett.*, 2014, **113**, 046804.
27 J. Liu, Y. Guo, S. Zhang, Q. Wang, Y. Kawazoe and P. Jena, *J. Phys. Chem. C*, 2015, **119**, 24674–24680.

28 W. Kohn and L. J. Sham, *Phys. Rev.*, 1965, **140**, A1133–A1138.
29 G. Kresse and J. Furthmüller, *Phys. Rev. B: Condens. Matter*, 1996, **54**, 11169–11186.
30 J. P. Perdew, K. Burke and M. Ernzerhof, *Phys. Rev. Lett.*, 1996, **77**, 3865–3868.
31 S. Grimme, C. Muck-Lichtenfeld and J. Antony, *J. Phys. Chem. C*, 2007, **111**, 11199–11207.
32 S. Grimme, *J. Comput. Chem.*, 2006, **27**, 1787–1799.
33 N. Kharche and S. K. Nayak, *Nano Lett.*, 2011, **11**, 5274–5278.
34 A. Togo, F. Oba and I. Tanaka, *Phys. Rev. B: Condens. Matter*, 2008, **78**, 134106.
35 J. Zhou and R. Huang, *J. Mech. Phys. Solids*, 2008, **56**, 1609–1623.
36 F. Mouhat and F. Coudert, *Phys. Rev. B: Condens. Matter*, 2014, **90**, 224104.
37 A. H. Reshak and M. Jamal, *J. Alloys Compd.*, 2012, **543**, 147–151.
38 P. Ravindran, L. Fast, P. A. Korzhavyi, B. Johansson, J. Wills and O. Eriksson, *J. Appl. Phys.*, 1998, **84**, 4891.
39 P. W. O. Nyawere, N. W. Makau and G. O. Amolo, *Phys. Rev. B: Condens. Matter*, 2014, **434**, 122–128.
40 A. Marmier, Z. A. D. Lethbridge, R. I. Walton, C. W. Smith, S. C. Parker and K. E. Evans, *Comput. Phys. Commun.*, 2010, **181**, 2102–2115.
41 F. Liu, P. Ming and J. Li, *Phys. Rev. B: Condens. Matter*, 2007, **76**, 064120.
42 C. Si, W. Duan, Z. Liu and F. Liu, *Phys. Rev. Lett.*, 2012, **109**, 226802.
43 C. A. Marianetti and H. G. Yevick, *Phys. Rev. Lett.*, 2010, **105**, 245502.
44 J.-C. Tan, B. Civalleri, A. Erba and E. Albanese, *CrystEngComm*, 2015, **17**, 375–382.
45 L. Song, L. Ci, H. Lu, P. B. Sorokin, C. Jin, J. Ni, A. G. Kvashnin, D. G. Kvashnin, J. Lou, B. I. Yakobson and P. M. Ajayan, *Nano Lett.*, 2010, **10**, 3209–3215.
46 C. Lee, X. Wei, J. W. Kysar and J. Hone, *Science*, 2008, **321**, 385–388.
47 A. Castellanos-Gomez, M. Poot, G. A. Steele, H. S. J. van der Zant, N. Agraït and G. Rubio-Bollinger, *Adv. Mater.*, 2012, **24**, 772–775.
48 J. Klimeš, D. R. Bowler and A. Michaelides, *Phys. Rev. B: Condens. Matter*, 2011, **83**, 195131.
49 J. Klimeš, D. R. Bowler and A. Michaelides, *J. Phys.: Condens. Matter*, 2010, **22**, 22201.
50 Y. Du, J. Maassen, W. Wu, Z. Luo, X. Xu and P. D. Ye, *Nano Lett.*, 2016, **16**, 6701–6708.
51 J. L. Zhang, S. Zhao, C. Han, Z. Wang, S. Zhong, S. Sun, R. Guo, X. Zhou, C. Gu, K. Yuan, Z. Li and W. Chen, *Nano Lett.*, 2016, **16**, 4903–4908.
52 E. Gao and Z. Xu, *J. Appl. Mech.*, 2015, **82**, 121012.